Preparation and Characterization of Cellulose Nanocrystal from Pineapple Leaves for Use in PLA/PBAT Composites

Nichakorn Pathumrangsan

Faculty of Science and Technology, Muban Chombueng Rajabhat University, Ratchaburi, Thailand. nichakornpat@mcru.ac.th

KEYWORDS
Blends, PBAT, Pineapple Leaves, PLA, Nanocellulose

ABSTRACT
This research involves utilizing CNCs technology derived from pineapple leaves to enhance the properties of polylactic acid (PLA) to create a nanocomposite film product with effective UV protection. It also examines the effects on other material properties, such as strength and flexibility, for practical applications of the polymer blend. The experimental process involves extracting nanocrystalline cellulose (CNCs) from pineapple leaves, which are treated through an alkali surface treatment, bleaching to remove lignin, and acid hydrolysis with sulfuric acid to obtain CNCs. The synthesized CNC are then used as a filler in polylactic acid (PLA), which is blended with polybutylene adipate terephthalate (PBAT). The mixture is then formed into nanocomposite films and tested for various properties.
The results showed that PLA/PBAT/CNCs films exhibited a reduction in mechanical properties, such as tensile strength and elongation at break. This reduction is primarily attributed to the agglomeration of CNCs, leading to uneven distribution within the PLA/PBAT matrix, which inhibits effective stress transfer across the material. When the films were tested for UV absorption properties, it was found that the PLA film allowed light to pass through in the wavelength range of 200-224 nm, allowing both UV and visible light to transmit. In contrast, the nanocomposite PLA films exhibited reduced light transmission, indicating that CNCs either absorb or scatter UV light effectively, enhancing UV protection capabilities. Regarding the thermal stability of the PLA and PLA nanocomposite films, adding CNCs to PLA caused the recrystallization temperature (T_{cc}) to decrease, indicating slower molecular arrangement. At the same time, The melting temperature (T_m) increased when CNCs were added, showing multiple melting behaviors. This phenomenon suggests the presence of different crystalline structures or phases due to the heterogeneous distribution of CNCs within the PLA matrix. The presence of two melting temperature peaks indicates the incompatibility between PLA/PBAT and CNCs.

1. Introduction:

Plastics are essential raw materials extensively used in producing a wide range of products, including agricultural tools, medical supplies, packaging, and everyday items. These plastics are predominantly derived from petroleum-based polymers, which are non-biodegradable and thus unable to break down naturally. Consequently, they contribute significantly to environmental waste problems. In response, a growing interest has been in creating biobased and biodegradable polymers to replace petroleum-based plastics. Poly(lactic acid) or PLA, for instance, is a renewable, bio-based, and biodegradable thermoplastic polyester, commonly produced from plants such as cassava, sugarcane, and corn [1-4]. The advantage properties of PLA are high strength and high modulus that use in either the industrial packaging field or the biocompatible medical device [5]. However, PLA lacks some important characteristics like flexibility, melt strength, and fast crystallization rate [6]. To overcome this limitation, blends of PLA with poly(butylene adipate-co-terephthalate) (PBAT) have been developed, as PBAT provides enhanced flexibility and toughness.

The incorporation of PBAT into PLA can enhance certain characteristics of the polymer, though it may also compromise the strength and modulus of the blend. In recent years, extensive research has focused on adding nanoparticles to these immiscible polymer blends to achieve superior physical properties. The selective placement of nanoparticles like nanoclay [7-10], graphene [11-12], carbon nanotubes [13-14], nano-silica [15-16] and cellulose nanocrystals [17-18] within PLA/PBAT blends has been shown to yield a range of optimized morphologies, each imparting unique benefits. For example, nanoclay strengthens the blend by stabilizing PBAT droplet dispersion, while graphene and carbon nanotubes localize within the PBAT phase to create robust percolated networks. Meanwhile, nano-silica's positioning can shift the blend structure, enhancing elongation and impact resistance when used in higher concentrations. This strategic nanoparticle integration thus offers an effective means of tailoring polymer blend properties for specific applications.

In recent years, cellulose nanocrystals (CNCs) have gained significant attention as reinforcing agents due to their exceptional mechanical properties and biocompatibility. Extracted from natural sources such as pineapple leaves, CNC offers a sustainable solution for improving the performance of polymer blends. Pineapple leaves, an agricultural byproduct, are abundant and represent an untapped resource for CNC extraction. CNC is hydrophilic and one-dimensional (1D) fibrous material. This could bring about CNC agglomerations in a polymer matrix when simultaneous melt mixing methods are used [19–20]. Therefore, the solvent dissolution is shown to be one of the most efficient methods to disperse CNC in polymers such as PLA and PBAT [21–23]. It has been reported that a combination of solution casting and melt mixing methods may result in a good level of CNC dispersion in PLA and PBAT. Mohammadi et al. [24] explored the localization of CNCs in PLA (amorphous and semicrystalline)/PBAT blend nanocomposites.

Corresponding nanocomposites were prepared through firstly solution casting with different mixing strategies, and then melt mixing using an internal mixer. Regardless of the initial localization of the CNCs, they were found to be inside the PBAT droplets. This in turn, led to PBAT droplet size reduction and finer morphology in the blend nanocomposites.

This study focuses on the preparation and characterization of CNC extracted from pineapple leaves for incorporation into PLA/PBAT blends. By examining the effects of varying CNC concentrations on the physical and mechanical properties of the resulting composites, this research aims to enhance the overall performance of PLA/PBAT blends while promoting the use of renewable materials. The findings of this work could contribute to the development of sustainable, high-performance materials suitable for various applications, including packaging and consumer products.

2. Objectives

This study aims to extract and characterize cellulose nanocrystals (CNCs) from pineapple leaves for incorporation into PLA/PBAT blends as a reinforcing agent. By varying the CNC concentrations, the research seeks to evaluate their effects on the physical and mechanical properties of the resulting composites. Additionally, this study aims to enhance the overall performance and sustainability of PLA/PBAT blends by utilizing renewable CNCs, contributing to the development of biodegradable polymer materials suitable for various applications.

3. Materials And Methods

Materials

A commercial grade of PLA (Ingeo 4043D) was supplied from Naturework LLC. The weight average molecular weight of 2.10 x 105 g/mol and polydispersity of 1.6. The neat polymer granules are pre-dried at 60oC for overnight before use.

The PBAT (Ecoflex® F Blend C1200) that is a grade for blown or cast film processing was supplied from BASF. That show a weight average molecular weight of 1.05 x 105 g/mol and a polydispersity of 2.0.

The pineapple leaves that used for synthesizing CNCs was supplied from amphoe Bankha, Ratchaburi in Thailand. 97% purity sodium hydroxide (NaOH) was purchased from Ajax Finechem. 10% (w/v) sodium chlorite (NaClO2) was purchased from local industry in Thailand. Acetic acid (CH3COOH) was purchased from Quality Reagent chemical. 98% sulfuric acid (H2SO4) was purchased from Merck, Germany.

Methods

Extraction of cellulose

First, pineapple leaves were washed and chopped to small size, dried them in oven at 90ºC, and grinded into pineapple leave powder. After that, the cellulose was extracted from pineapple leave powder by

alkali treatment 2 times by using 30 g of pineapple leave powder to 600 ml of 1 % w/v NaOH at 80°C for 2 hrs under stirring condition. Then, bleaching treatment was carried out three times using 0.7 %w/v NaClO2 at 80°C for 1 hr using the ratio of material to liquid was 1:20 (g/ml). At the end the cellulose was neutralize by distilled water and dried in oven at 70°C overnight

Acid Hydrolysis

The CNCs were produced by hydrolyzing the extracted cellulose with acid hydrolysis method. First, 1 g of extracted cellulose was added into 20 ml of 64 %w/w sulfuric acid to form a suspension. It was continued hydrolyzed at 45°C for 3 hr. At the end of reaction, the suspension product was filled with 10 fold water for stop reaction and then centrifuged at 7,500 rpm for 10 min to separate the gel suspension and remove the excess acid. The gel was adjusted to neutral by filtering through dialysis membrane and immersed in water. Finally, neutral gel was sonicated by ultrasonic sonicator.

Preparation of blend nanocomposites

In this study, PLA/PBAT/CNC blend nanocomposites containing varying amounts of CNC (1, 2.5, 5, and 7.5 wt%) were prepared using the solution casting (SC) method. First, PLA and PBAT were weighed according to the amounts shown in Table 1 and then added to 150 ml of chloroform. The mixtures were stirred vigorously on a magnetic stirrer at 70°C for 2.5 hours, ensuring both polymers were fully dissolved. The mixtures were eventually poured into petri dishes and dried in a hood at room temperature for two days.

Table 1. The ratios of PLA/PBAT/CNC blends

Sample code	%PLA	%PBAT	%CNC
F1	100	0	0
F2	80	20	0
F3	***80***	***19***	***1***
F4	***80***	***17.5***	***2.5***
F5	***80***	***15***	***5***
F6	***80***	***12.5***	***7.5***

Characterization

1) Characterization of synthesized CNC

The synthesized CNC was characterized unctional group by fourier transformed infrared spectroscopy (FT-IR) [25]. The XRD pattern of samples was recorded to calculate crystallinity index (C_I) by using (1).

$$C_I = (I_{002} - I_{am})/ I_{002} \quad (1)$$

When, I_{002} represented the maximum intensity of parts of crystalline and amorphous at $2\theta = 22^o$, and I_{am} is the intensity peak of only amorphous region at 2θ around 18^o.

2) Characterization of PLA/PBAT/CNC blend nanocomposites

-Differential Scanning Calorimetry analysis

The thermal behaviors of blend and blend nanocomposites were explored using a DSC, Q2000, TA Instrument under nitrogen atmosphere. The samples was expose to heat/cool/heat cycles between 25 - 200^{o}C. The heating rate for heating cycles is 10^{o}C/min and the cooling rate for cooling cycle is 2^{o}C/min.

-Machanical analysis

Tensile strength and elongation at break of blend and blend nanocomposites were analyzed using an Instron 8801device. Tensile properties were determined according to the ASTM D882-18 method [26]. Films were cut into 10 mm wide strips and at least 120 mm long. The grip separation and crosshead

speed were 50 mm and 500 mm/min, respectively. At least five specimens were tested for each sample.

-UV absortion analysis

The UV absorption properties of the films were evaluated by measuring the absorption spectrum within the 200-800 nm range using a UV/visible spectrophotometer (Model U-2900, Hitachi). The UV absorption of the films was compared by examining the variations in peak intensity within the 200-400 nm range. To determine which groups exhibited statistically significant differences, A one-way analysis of variance (ANOVA) was conducted at a 95% confidence level using SPSS software (version X.X) to determine statistically significant differences.

4. Results And Discussion

Functional groups of synthesized CNCs by FT-IR

Nanocrystalline cellulose, following the final extraction stage, forms a white, cloudy suspension. This suspension is subsequently analyzed using FTIR (Fourier-transform infrared spectroscopy) to verify its chemical structure. A comparison was made between the extracted nanocrystalline cellulose (CNCs), pineapple leaf fibers bleached by sulfuric acid hydrolysis (PAL-B), and unprocessed dry pineapple leaves (PAL), as illustrated in Figure 1.

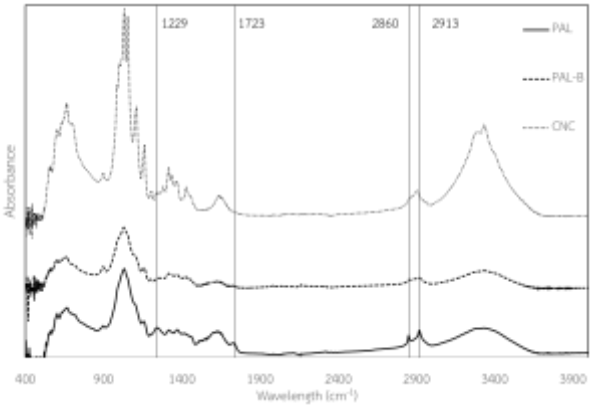

Figure 1. The infrared absorption spectra of dry pineapple leaf (PAL), bleached dry pineapple leaf (PAL-B), and nanocrystalline cellulose (CNCs).

The analysis revealed that all spectra exhibited infrared absorption in the 3000 to 3500 cm^{-1} range, attributed to O-H stretching. At 2913 cm^{-1} and 2860 cm^{-1}, C-H stretching of cellulose molecules was observed [27]. In the unprocessed dry pineapple leaf (PAL), C=O stretching of α, β-unsaturated ester compounds was detected at 1723 cm^{-1}, along with C-O stretching at 1230 cm^{-1}, which corresponds to symmetrical ether groups indicating lignin presence. The absence of peaks at 1723 cm^{-1} and 1230 cm^{-1} in the bleached pineapple leaf fiber (PAL-B) spectrum suggests the complete removal of hemicellulose and lignin [28]. The peak at 1115 cm^{-1} is indicative of asymmetric C-O-C stretching within the six-membered ring, while the peak at 896 cm^{-1} is related to the CH bond rocking of cellulose [29]. Generally, the intensity of these peaks is directly proportional to the cellulose content.

The crystal structure analysis of bleached dry pineapple leaf (PAL-B) and CNCs using X-ray Diffraction (XRD)

After analyzing the chemical structure of bleached dry pineapple leaf (PAL-B) and nanocrystalline cellulose (CNCs) using FTIR, the crystal structure of these materials was studied using X-ray Diffraction (XRD). This technique relies on the principle of X-ray diffraction, where the X-rays strike the sample and are scattered, producing reflected rays at angles equal to the incident rays. Figure 2 shows the XRD graph for bleached pineapple leaf (PAL-B) and CNCs. The results indicate that the crystal structure analyzed corresponds to cellulose type I (Cellulose I), which is typically found in plants and biosynthesized by bacteria. Peaks were observed at approximately 15° (plane 110), 22°

(plane 002), and 35° (plane 004) [30].

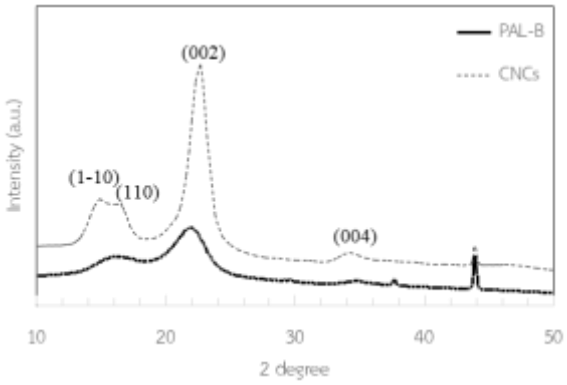

Figure 2. XRD patterns of bleached dry pineapple leaf (PAL-B) and nanocrystalline cellulose (CNCs).

The peak around 22° represents the interlayer spacing in the 3D stack structure, held together by Van der Waals forces. Each 2D layer is formed by cellulose molecules connected through intra- and intermolecular hydrogen bonds. This complex hydrogen bonding network, along with Van der Waals forces between molecules, regulates the cellulose chains, leading to the formation of a semi-crystalline polymer. Cellulose I is the dominant natural structure, comprising two crystalline forms: Cellulose Iα, with a triclinic structure, and Cellulose Iβ, with a monoclinic structure [31, 32]. The XRD spectrum for CNCs also shows a peak overlap near 16.5°, representing the (1-10) and (110) planes, due to the two lattice constants of the cellulose crystals [31].

The crystallinity index of CNCs and PAL-B was determined to be 75.31% and 26.27%, respectively, calculated using Equation (1). The hydrolysis process using sulfuric acid during CNCs production leads to the modification of the chemical structure of the cellulose chains. This occurs due to the absorption of hydrogen ions (H^+ ions) from the acid, which simultaneously removes the amorphous regions and lignin from the cellulose, resulting in a higher crystallinity index for CNCs compared to PAL-B.

Thermal property analysis and phase transition temperatures of PLA nanocomposites using Differential Scanning Calorimetry (DSC)

The study on the influence of adding CNCs on the non-isothermal thermal behavior of PLA is presented in Figure 3, which shows the heat flow of PLA/CNCs samples as temperature increases. This relationship helps determine the phase transition temperatures of the polymer, as summarized in Table 2.

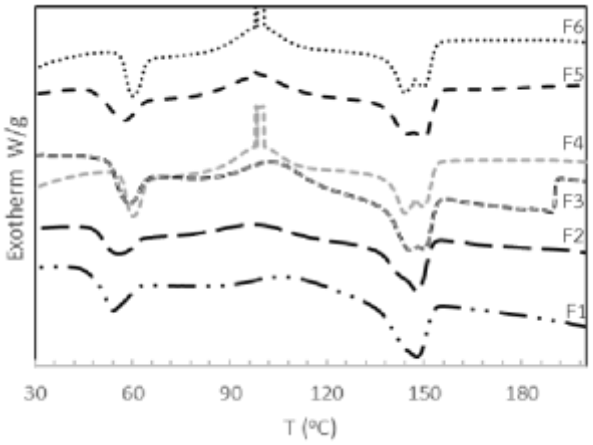

Figure 3. DSC curves of blends film in each formular that shows in Table 1

Table 2. DSC results of blend films in each formula

Sample code	T_g (°C)	T_{cc} (°C)	T_{m1} (°C)	T_{m2} (°C)
F1	55.50	108.50	147.70	-
F2	57.00	100.67	147.90	-
F3	60.50	105.16	144.70	149.40
F4	60.00	101.67	147.60	-
F5	58.00	99.17	145.20	149.70
F6	60.50	101.67	144.30	149.80

From the experiment, the glass transition temperature (T_g) and melting temperature (T_m) of the PLA film (formulation F1) were found to be 60.50°C and 147.70°C, respectively. The Tg of the F2 film (57.00°C) was similar to that of PLA, indicating no significant improvement in chain mobility when PBAT was blended with PLA, consistent with the findings of Su et al. [33]. For the nanocomposite films, Tg increased by approximately 3°C compared to the PLA/PBAT polymer film.

The cold crystallization temperature (T_{cc}) of the PLA film was 108.50°C. In PLA/PBAT nanocomposite films, the T_{cc} decreased as the CNCs content (ranging from 1-5%) increased. This is because the small CNC crystals can penetrate the polymer chains and disrupt the crystallization process, making it harder for the polymer to arrange itself, thus lowering the Tcc and slowing down crystallization.

As for the melting temperature (Tm), the PLA film and PLA nanocomposite films showed the values listed in Table 2. The PLA film had a Tm of 147.70°C, which was a single peak, whereas the PLA/PBAT nanocomposite films exhibited two melting peaks, labeled as T_{m1} and T_{m2}. The appearance of these two peaks is due to defects in the molecular chains, directly affecting the crystallization of PLA. CNCs influence crystallization within the structure, causing crystals of varying sizes, which indicates imperfections or inconsistencies in the crystalline structure. The Tm1 peak is influenced by the added filler, while the T_{m2} peak is related to the melting of PLA crystals.

Mechanical properties of blends and blend nanocomposites.

The mechanical properties of PLA films and PLA/PBAT nanocomposite films were tested using a Universal Testing Machine (UTM) according to ASTM D882. The films were cut into 25 x 100 mm samples, and the tensile testing speed was set at 5 mm/min. The test results are summarized in Table 3.

Table 3. Mechanical properties of blend and blend nanocomposites

Sample code	**Tensile strength (MPa)**	**Elongation at break (%)**

F1 (pure PLA) (Control)	51.5	2.53
F2	37.3	3.43
F3	37.9	2.54
F4	35.0	2.15
F5	37.0	2.20
F6	26.5	2.46

The results in Table 3 show that as the CNC content increases (formulations F3-F6), both the tensile strength and elongation at break decrease. This may be attributed to the agglomeration of CNC particles, which have hydrophilic hydroxyl (-OH) groups. The increased hydrophilicity causes CNCs to cluster together, leading to uneven dispersion within the PLA/PBAT matrix. As a result, the mechanical properties are reduced compared to the PLA film (F1).

Optical transmittance of blend and blend nanocomposites

The visual characteristics of blend nanocomposites, F1 to F6, indicate that the PLA film is transparent, allowing objects to be clearly seen through it. However, when PLA is blended with PBAT and further combined with CNCs, the light transmission through the film decreases. Analysis of the UV spectrum in the range of 200-800 nanometers reveals that the PLA film permits light transmission in the wavelength range of 200-224 nanometers, allowing both UV and visible light to pass through.

In contrast, the PLA nanocomposite films show reduced light transmission as the CNC content increases. These films do not allow UV light to pass through but permit visible light to do so, indicating a significant change in their optical properties due to the incorporation of CNCs.

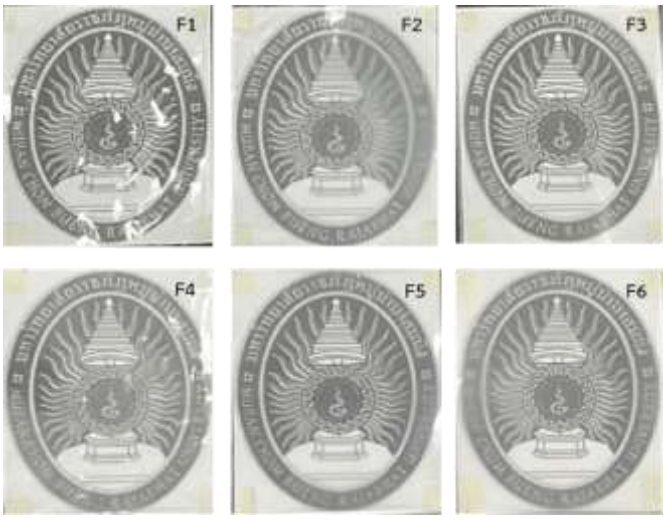

Figure 4. PLA film and blend nanocomposites by casting method

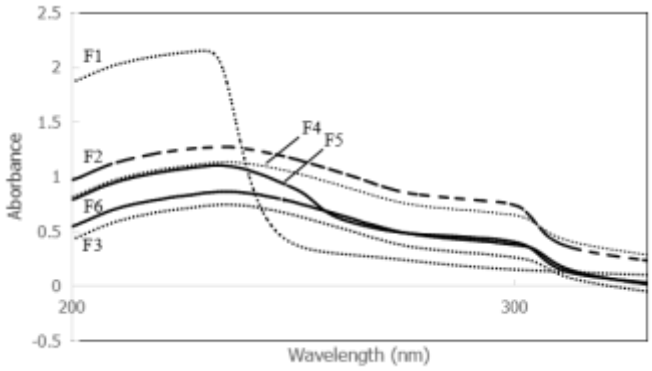

Figure 5. Spectrum of PLA film and blend nanocomposites in 200 - 330 nm.

Table 4. The light absorption at the peak wavelengths of the sample films.

Sample Code	Ratio			Wavelength (nm)	Abs.
	PLA	PBAT	CNCs		
F1	100	0	0	219	2.0962
F2	80	20	0	224	1.2361
F3	80	19	1	223	0.6235
F4	80	17.5	2.5	227	1.0769
F5	80	15	5	223	1.0502
F6	80	12.5	7.5	227	0.8289

When comparing the light absorption values of the films from formulations 3 to 6 against those of formulations 1 and 2, as shown in Table 4, it was found that with a significance level of 0.05 and degrees of freedom (df) equal to 3, the t-critical value is 3.182 for a two-tailed test. For the comparison with sample 1, the calculated t-value is 11.29, which exceeds the t-critical value of 3.182. Therefore, this difference is significant at the 0.05 level. In the comparison with sample 2, the calculated t-value is 3.30, also greater than the t-critical value of 3.182. Consequently, this difference is significant at the 0.05 level as well.

5. Conclusion

The findings of this research indicate the successful synthesis of cellulose nanocrystals (CNCs) from pineapple fibers, which serve as a promising additive for PLA/PBAT polymer blends. The study meticulously details the manufacturing process, revealing the chemical transformations that enhance the crystallinity and purity of the cellulose extracted. The compatibility of CNCs with the PLA/PBAT blend was assessed through thermal analysis, showing modifications in thermal properties and crystallization behavior, which underscores the interaction between the nanocrystals and the polymer matrix. Mechanical tests demonstrated a decrease in tensile strength and elongation at break in the nanocomposite films, attributed to the agglomeration of CNCs. Furthermore, the optical properties of the films were analyzed, revealing a reduction in light transmission with increasing CNC content. These results collectively underscore the potential of incorporating CNCs from pineapple fibers to optimize the performance characteristics of biodegradable polymer films, contributing to sustainable materials development.

Acknowledgements

This research was funded by Muban Chombueng Rajabhat University.

Reference

[1] Chen, Y., Geever, L. M., Killion, J. A., Lyons, J. G., Higginbotham, C. L., and Devine, D. M., 2016, Review of multifarious applications of poly (lactic acid). *Polymer-Plastics Technology and Engineering*, 55 (10), 1057-1075.

[2] Garlotta, D., 2001, A literature review of poly (lactic acid). *Journal of Polymers and the Environment*, 9 (2), 63-84.

[3] Sinclair, R. G., 2013, The case for polylactic acid as a commodity packaging plastic. *Journal of Macromolecular Science, Part A: Pure and Applied Chemistry*, 33 (5), 585-597.

[4] Zhao, X., Hu, H., Wang, X., Yu, X., Zhou, W., and Peng, S., 2020, Super tough poly (lactic acid) blends: A comprehensive review. *RSC advances*, 10 (22), 13316-13368.

[5] Ouchi, T., and Ohya, Y., 2003, Design of lactide copolymers as biomaterials. *Journal of Polymer Science Part A: Polymer Chemistry*, 42 (3), 453-462.

[6] Nofar, M., Sacligil, D., Carreau, P. J., Kamal, M. R., and Heuzey, M. C., 2018, Poly (lactic acid) blends: Processing, properties and applications. *International journal of biological macromolecules*, 125, 307-360.

[7] Nofar, M., Salehiyan, R., Ciftci, U., Jalali, A., and Durmuş, A., 2020, Ductility improvements of PLA-based binary and ternary blends with controlled morphology using PBAT, PBSA, and nanoclay. *Composites Part B: Engineering*, 182,107661.

[8] Nofar, M., Heuzey, M. C., Carreau, P. J., Kamal, M. R., and De Pinho, M. N., 2020, Nanoparticle interactions and molecular relaxation in PLA/PBAT/nanoclay blends. *Experimental Results*, 1, 1-12.

[9] Nofar, M., Heuzey, M. C., Carreau, P. J., and Kamal, M. R., 2016, Effects of nanoclay and its localization on the morphology stabilization of PLA/PBAT blends under shear flow. *Polymer*, 98, 353-364.

[10] Jiang, L., Liu, B., and Zhang, J., 2009, Properties of poly (lactic acid)/poly (butylene adipate-co-terephthalate)/nanoparticle ternary composites. *Industrial & Engineering Chemistry Research*, 48, 7594-7602.

[11] Adrar, S., Habi, A., Ajji, A., and Grohens, Y., 2018, Synergistic effects in epoxy functionalized graphene and modified organo-montmorillonite PLA/PBAT blends. *Applied Clay Science*, 157, 65-75.

[12] Girdthep, S., Komrapit, N., Molloy, R., Lumyong, S., Punyodom, W. and Worajittiphon, P., 2015, Effect of plate-like particles on properties of poly (lactic acid)/poly (butylene adipate-co-terephthalate) blend: A comparative study between modified montmorillonite and graphene nanoplatelets. *Composites Science and Technology*, 119, 115-123.

[13] Ko, S. W., Hong, M. K., Park, B. J., Gupta, R. K., Choi, H. J., and Bhattacharya, S. N., 2009, Morphological and rheological characterization of multi-walled carbon nanotube/PLA/PBAT blend nanocomposites. *Polymer bulletin*, 63, 125-134.

[14] Urquijo, J., Aranburu, N., Dagréou, S., Guerrica-Echevarría, G., and Eguiazábal, J. I., 2017, CNT-induced morphology and its effect on properties in PLA/PBAT-based nanocomposites. *European Polymer Journal*, 93, 545-555.

[15] Dil, E. J., and Favis, B. D., 2015, Localization of micro-and nano-silica particles in heterophase poly (lactic acid)/poly (butylene adipate-co-terephthalate) blends. *Polymer*, 76, 295-306.

[16] Dil, E. J., Virgilio, N., and Favis, B. D., 2016, The effect of the interfacial assembly of nano-silica in poly (lactic acid)/poly (butylene adipate-co-terephthalate) blends on morphology, rheology and mechanical properties. *European Polymer Journal*, 85, 635-646.

[17] Mohammadi, M., Heuzey, M. C., Carreau, P. J., and Taguet, A., 2017, Morphological and rheological properties of PLA, PBAT, and PLA/PBAT blend nanocomposites containing CNCs. *Nanomaterials*, 11(4), 857.

[18] Sarul, D. S., Arslan, D., Vatansever, E., Kahraman, Y., Durmus, A., Salehiyan, R. and Nofar, M., 2021, Preparation and characterization of PLA/PBAT/CNC blend nanocomposites. *Colloid and Polymer Science*, 299, 987-998.

[19] Nuzzo, A., Bilotti, E., Peijs, T., Acierno, D., and Filippone, G., 2014, Nanoparticle-induced co-continuity in immiscible polymer blends–A comparative study on bio-based PLA-PA11 blends filled with organoclay, sepiolite, and carbon nanotubes. *Polymer*, 55, 4908-4919.

[20] Wu, G., Li, B., and Jiang, J., 2010, Carbon black self-networking induced co-continuity of immiscible polymer blends. *Polymer*, 51, 2077-2083.

[21] Elias, L., Fenouillot, F., Majesté, J. C., Martin, G., and Cassagnau, P., 2008, Migration of nanosilica particles in polymer blends. *Journal of Polymer Science Part B: Polymer Physics*, 46, 1976-1983.

[22] Elias, L., Fenouillot, F., Majesté, J. C., and Cassagnau, P., 2007, Morphology and rheology of immiscible polymer blends filled with silica nanoparticles. *Polymer*, 48, 6029-6040.

[23] Elias, L., Fenouillot, F., Majesté, J. C., Alcouffe, P., and Cassagnau, P., 2008, Immiscible polymer blends stabilized with nano-silica particles: Rheology and effective interfacial tension. *Polymer*, 49, 4378-4385.

[24] Shahlari, M. and Lee, S., 2012, Mechanical and morphological properties of poly (butylene adipate-co-terephthalate) and poly (lactic acid) blended with organically modified silicate layers. *Polymer Engineering & Science*, 52, 1420-1428.

[25] Wang, L. F., Rhim, J. W., & Hong, S. I.,2016, Preparation of poly (lactide)/poly (butylene adipate-co-terephthalate) blend films using a solvent casting method and their food packaging application. *LWT-Food Science and Technology*, 68, 454-461.

[26] ASTM-D882, 2018. Standard test method for tensile properties of thin plastic sheeting, D882-18 West Conshohocken, PA

[27] Mandal, A. and Chakrabarty, D., 2011, Isolation of nanocellulose from waste sugarcane bagasse (SCB) and its characterization. *Carbohydrate polymers*, vol. 86, pp. 1291-1299, August 2011.

[28] Dos Santos, R. M., Neto, W. P. F., Silvério, H. A., Martins, D. F., Dantas, N. O., and Pasquini, D., 2013, Cellulose nanocrystals from

pineapple leaf, a new approach for the reuse of this agro-waste. *Industrial Crops and Products*, 50, 707-714.

[29] Haafiz, M. M., Hassan, A., Zakaria, Z. and Inuwa, I. M., 2014, Isolation and characterization of cellulose nanowhiskers from oil palm biomass microcrystalline cellulose. *Carbohydrate polymers*, 103, 119-125.

[30] Morán, J. I., Vazquez, A., and Cyras, V. P., 2013, Bio-nanocomposites based on derivatized potato starch and cellulose, preparation and characterization. *Journal of Materials Science*, 48, 7196-7203.

[31] French, A. D., 2013, Idealized powder diffraction patterns for cellulose polymorphs. *Cellulose*, 21, 885-896.

[32] Feng, H., Du, L., Liu, S., and Zhang, X., 2017, Effects of different deficit irrigation on sugar accumulation of pineapple during development. *In IOP Conference Series: Earth and Environmental Science*, 81, 012037.

[33] Su, S., Duhme, M., and Kopitzky, R., 2020, Uncompatibilized PBAT/PLA blends: manufacturability, miscibility and properties. *Materials*, 13, 4897.